Journal of Medicinal Chemistry

ARTICLE

pubs.acs.org/jmc

3-Hydroxypyrimidine-2,4-diones as an Inhibitor Scaffold of HIV Integrase

Jing Tang,[†] Kasthuraiah Maddali,[‡] Mathieu Metifiot,[‡] Yuk Y. Sham,[†] Robert Vince,[†] Yves Pommier,[‡] and Zhengqiang Wang*[,†]

[†]Center for Drug Design, Academic Health Center, University of Minnesota, Minneapolis, Minnesota 55455, United States

[‡]Laboratory of Molecular Pharmacology, National Cancer Institute, National Institutes of Health, Bethesda, Maryland 20892, United States

Supporting Information

ABSTRACT: Integrase (IN) represents a clinically validated target for the development of antivirals against human immunodeficiency virus (HIV). Inhibitors with a novel structure core are essential for combating resistance associated with known IN inhibitors (INIs). We have previously disclosed a novel dual inhibitor scaffold of HIV IN and reverse transcriptase (RT). Here we report the complete structure−activity relationship (SAR), molecular modeling, and resistance profile of this inhibitor type on IN inhibition. These studies support an antiviral mechanism of dual inhibition against both IN and RT and validate 3-hydroxypyrimidine-2,4-diones as an IN inhibitor scaffold.

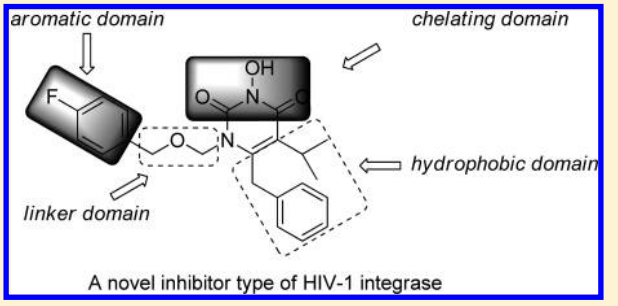

INTRODUCTION

HIV infection and the establishment of proviral latency depend critically on the insertion of viral DNA into host genome.[1−3] This integration process comprises two distinct steps: 3′ processing (3′P), in which a sequence-specific endonucleolytic cleavage of the viral DNA generates a CA-OH at the 3′ end, and strand transfer (ST), where the processed viral DNA is inserted into the host genome through a transesterification reaction using the 3′ CA-OH as the nucleophile.[4] The virally encoded enzyme IN catalyzes both reactions and thus represents an important target for HIV chemotherapeutic intervention. IN as an antiviral target is rendered particular attractive by the lack of host cellular counterpart. On the other hand, IN uses the same active site (DD35E motif) for both steps where either a viral DNA (in 3′P) or a cellular DNA (in ST) serves as the endogenous substrate. Therefore, inhibitors of IN could also benefit from a potentially high genetic barrier to resistance development. In the past two decades, IN-targeted antiviral research has led to the identification of various inhibitor types, of which the most prominent scaffolds all feature a diketoacid (DKA) functionality or its heterocyclic bioisosteres.[5−9] These chemotypes can accommodate highly selective ST inhibition and have played an essential role in unraveling the pharmacophore requirements for IN binding.[10−15] Extensive research on these chemotypes culminated with a number of investigational drugs (Figure 1), including raltegravir (**1**),[16,17] the first and only INI presently approved for clinical use, elvitegravir (**2**),[18] a promising candidate in phase III development, and S/GSK-1349572 (**3**),[19,20] a second-generation IN inhibitor in phase IIb trials.[21] In the meantime, HIV integration also involves a cellular cofactor

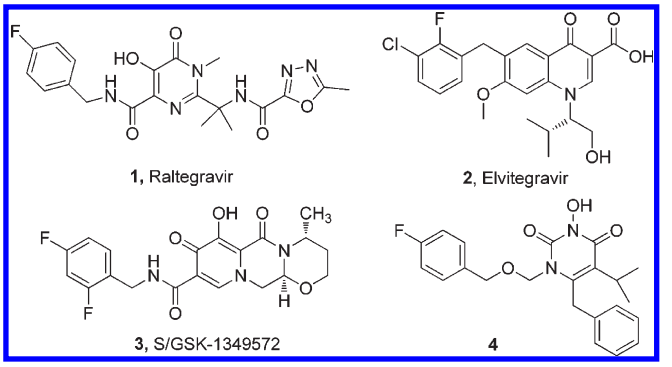

Figure 1. Structures of best known INIs (**1**−**3**) and a novel INI (**4**).

LEDGF/p75.[22−24] Targeting the protein−protein interaction between IN and LEDGF/p75 represents an emerging approach to HIV chemotherapeutic intervention.[25] Collectively, inhibitors targeting IN can substantially enhance the current highly active antiretroviral therapy (HAART), the standard chemotherapy for HIV/AIDS.[26] However, mutations conferring resistance to these inhibitors have been generated in cell culture and emerged in clinical studies,[27−29] suggesting that INIs will be confronted with the same resistance issue that has plagued HIV/AIDS chemotherapy. Continued search for structurally novel INIs to combat resistance is therefore urgently needed. Previously, we have reported that N-3 hydroxylation of pyrimidine-2,4-diones yielded inhibitors dually active against HIV reverse transcriptase (RT) and IN

Received: November 9, 2010
Published: March 07, 2011

(**4**, Figure 1).[30] Because this scaffold represents a novel chemotype for INIs, further SAR efforts on IN inhibition are warranted.

HIV IN is a 32 kDa protein encoded by viral pol gene consisting of three functional domains:[31] the N-terminal domain (NTD), with a conserved "HH−CC"zinc-binding motif, the catalytic core domain (CCD), containing the key D64-D116-E152 catalytic triad, and the C-terminal domain (CTD), important for DNA binding. Crystal structures of each single domain as well as double domains have been resolved,[32−34] albeit without the binding of viral DNA substrate. Detailed understanding on HIV IN catalysis requires structural information on a DNA-bound full-length IN complex, or an intasome, which currently remains elusive due to major technical barriers[35] in obtaining stable HIV intasome. Recently disclosed crystal structures of a homologous prototype foamy virus (PFV) intasome[36,37] have revealed the requisite catalytic molecular network comprising IN, viral, and/or host

Scheme 1. Synthesis of Aromatic and Chelating Domains[a]

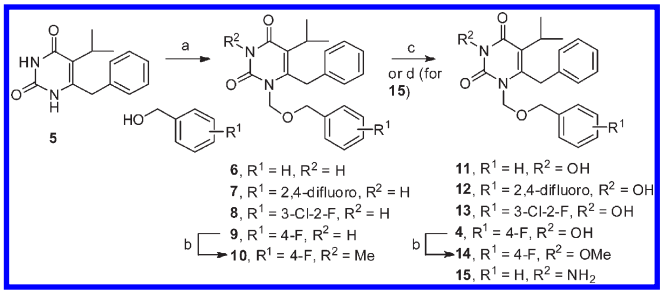

[a] Reagents and conditions: (a) $CH_3C(OTMS)$═NTMS (BSA), substituted benzyl alcohol, $(HCHO)_n$, TMSCl, TBAI (cat.), CH_2Cl_2, rt, 70−90%; (b) Cs_2CO_3, THF, MeI, 40 °C, 53−63%; (c) NaH, *m*-CPBA, THF, rt, 53−85%; (d) NaH, MSH, THF, rt, 54%.

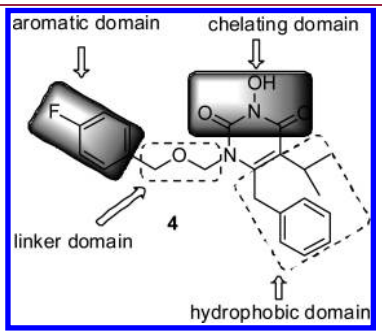

Figure 2. SAR design of lead compound **4**. Major structural domains are highlighted.

Scheme 2. Synthesis of Linker Domain[a]

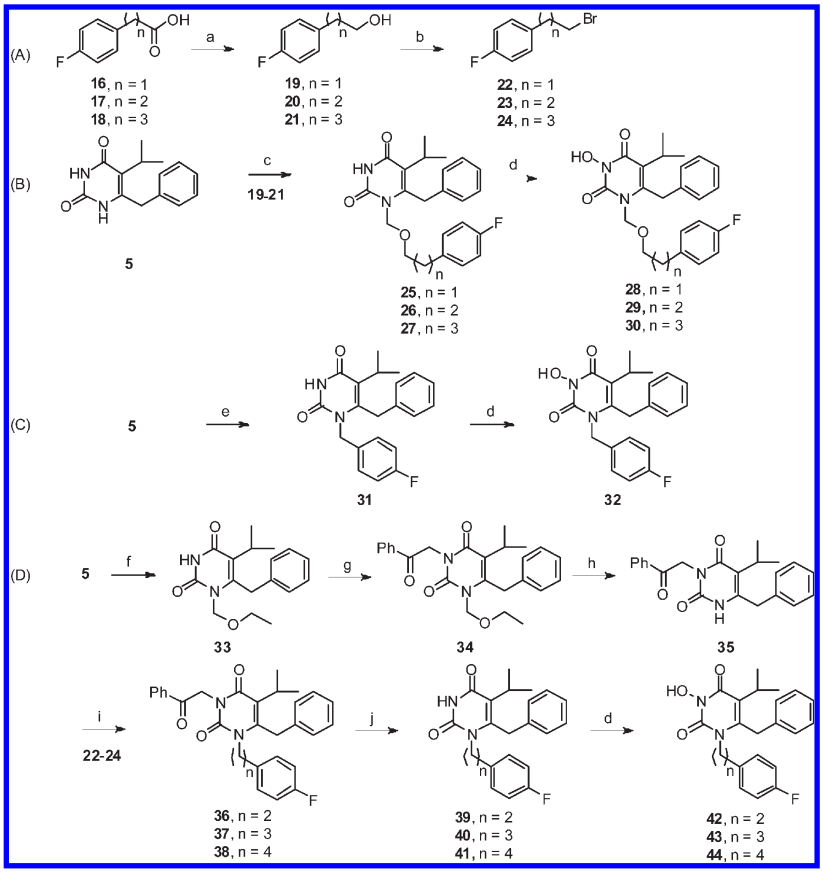

[a] Reagents and conditions: (a) $LiAlH_4$, THF, rt, 67−72%; (b) CBr_4, PPh_3, THF, rt, 73−80%; (c) $CH_3C(OTMS)$═NTMS (BSA), CH_2Cl_2; **19**−**21**, $(HCHO)_n$, TMSCl, TBAI (cat.), rt, 83−89%; (d) NaH, *m*-CPBA, THF, rt, 62−72%; (e) BSA, benzyl bromide, chlorobenzene, microwave, 160 °C, 50%; (f) BSA, chloromethyl ethyl ether, TBAI (cat.), CH_2Cl_2, rt, 89%; (g) K_2CO_3, $PhCOCH_2Br$, MeCN, reflux, 84%; (h) TFA:H_2O (9:1), reflux, 76%; (i) Cs_2CO_3, 4-F-Ph$(CH_2)_n$Br, DMF, 80 °C, 31−63%; (j) Mg, AcOH, MeOH, rt, 48−57%.

dx.doi.org/10.1021/jm1014378 |*J. Med. Chem.* 2011, 54, 2282–2292

Scheme 3. Synthesis of Hydrophobic Domain[a]

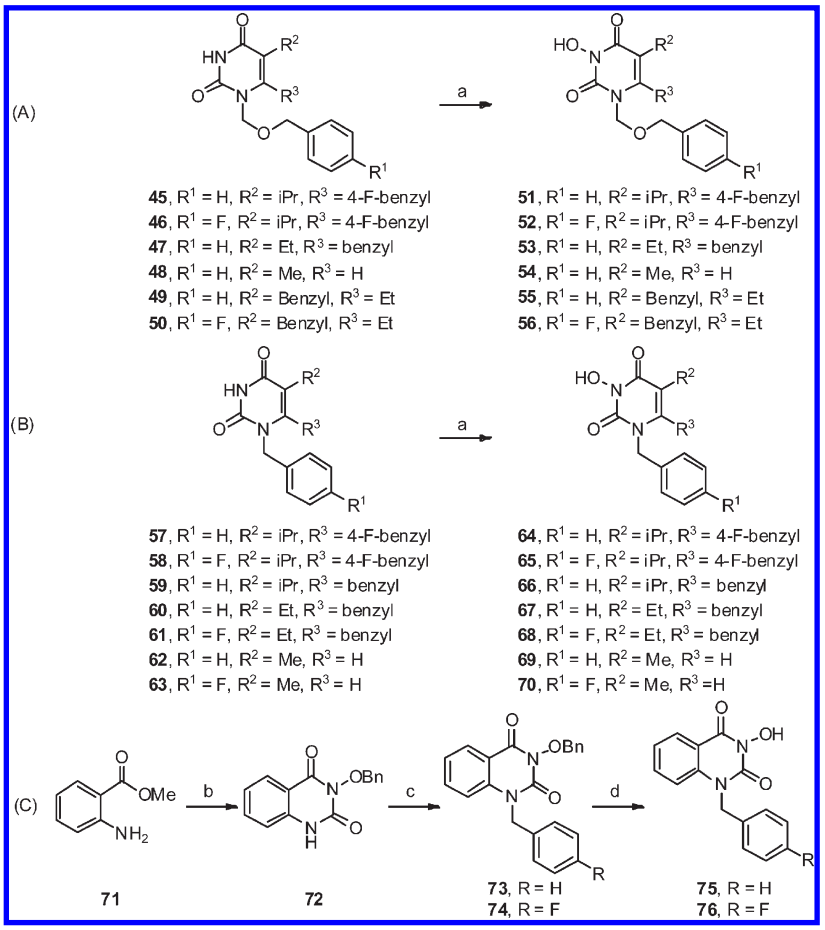

[a] Reagents and conditions: (a) NaH, *m*-CPBA, THF, rt 32−72%; (b) (i) CDI/toluene, reflux, then NH_2OBn, reflux, (ii) NaOH/EtOH, reflux, 53%; (c) benzyl bromide or 4-fluorobenzyl bromide, Cs_2CO_3, DMF, 80 °C, 58−67%; (d) HBr (48% in H_2O), reflux, 77−78%.

DNA substrates and the inhibitor, allowing a largely improved understanding on the mechanism of catalysis and inhibition of retroviral IN. Homologous models[38,39] constructed based on these PFV crystal structures have provided valuable details into HIV IN mechanism of action and formed the basis for structure-based INI design. Significantly these models corroborate the minimal pharmacophore embedded in major INIs: a chelating triad capable of binding two Mg^{2+} ions and a hydrophobic benzyl moiety. Our novel IN inhibitors are constructed around a pyrimidine-2,4-dione ring, a pharmacophore core that has found wide applications in medicinal chemistry.[40−43] Central to our design is to introduce an OH group on the N-3 position which, along with the two flanking carbonyl groups, would yield a chelating triad of C(O)N(OH)C(O) that mimics a DKA functionality (Figure 2, chelating domain). On the other hand, the hydrophobic benzyl moiety can be easily installed via an N-1 alkylation, and the mono- or dihalogenation of this terminal benzyl group will allow us to explore the halogen effect IN inhibition (Figure 2, aromatic domain). Furthermore, to ensure that this benzyl group can fit in the hydrophobic cavity, its spatial placement over the chelating triad has to be optimized. This can be achieved through a linker of different length (Figure 2, linker domain). Finally, the overall hydrophobicity of the inhibitor could be modified by altering the C5 and C6 substituents (Figure 2, hydrophobic domain).

RESULTS AND DISCUSSION

Chemistry. The chemical synthesis of aromatic and chelating domains starts with a known 5,6-disubstituted pyrimidine-2,4-dione **5**[44,45] (Scheme 1). Subsequent selective N-1 alkylation of **5** via a bis-silylated pyrimidine intermediate with an in situ generated chloromethyl ether allows the incorporation of the aromatic domain with an ether linkage (**6**−**10**, Scheme 1). As previously reported,[30] the key N-3 hydroxylation was achieved via a base-mediated *meta*-chloroperbenzoic acid (*m*-CPBA) oxidation. To assess the significance of this hydroxyl group on IN inhibition, an N-3 amino analogue (**15**) as well as analogues with an N-3 methyl or methoxy group were also synthesized (**10** and **14**, Scheme 1).

The synthesis of the linker domain is described in Scheme 2. Analogues with an ether linkage were easily prepared through a selective N-1 alkylation with a chloromethyl ether (Scheme 2B). The requisite alcohols (**19**−**21**) were synthesized from commercial carboxylic acids via a direct reduction with LAH. The construction of all-carbon tethers in the linker domain, however, proved much more challenging. The BSA-assisted selective N-1 alkylation of pyrimidine-2,4-diones generally involves a chloromethyl ether as the alkylating agent. The same reaction with benzyl bromide was effected only under forcing conditions (microwave, high temperature, and long reaction time; see Scheme 2C).

dx.doi.org/10.1021/jm1014378 |*J. Med. Chem.* 2011, 54, 2282–2292

Table 1. Effects of Aromatic and Chelating Domains on IN Inhibition

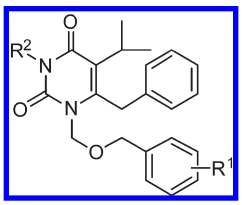

compd	R^1	R^2	IN IC_{50} (μM)[a] 3′P	ST[b]
11[c]	H	OH	>111	21 ± 2
12	2,4-F	OH	>111	4.8 ± 0.7
13	3-Cl-2-F	OH	>111	2.3 ± 0.6
4[c]	4-F	OH	>111	3.5 ± 0.6
9	4-F	H	>111	>111
10	4-F	Me	>111	>111
14	4-F	OMe	>111	>111
15[c]	H	NH_2	>111	>111

[a] Concentration inhibiting enzymatic function by 50%. [b] Mean value ± standard deviation from triplicate experiments. [c] Reference 30.

Table 2. Effects of Linker Domain on IN Inhibition

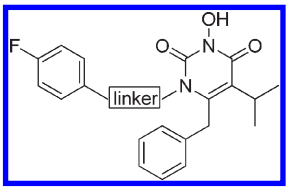

compd	linker	IN IC_{50} (μM)[a] 3′P	ST[b]
4[c]	CH_2OCH_2	>111	3.5 ± 0.6
28	$(CH_2)_2OCH_2$	>111	1.6 ± 0.2
29	$(CH_2)_3OCH_2$	>111	3.2 ± 0.5
30	$(CH_2)_4OCH_2$	>111	4.5 ± 0.4
32	CH_2	>111	22 ± 0.5
42	$(CH_2)_2$	>111	46 ± 6
43	$(CH_2)_3$	>111	0.44 ± 0.1
44	$(CH_2)_4$	>111	0.56 ± 0.04

[a] Concentration inhibiting enzymatic function by 50%. [b] Mean value ± standard deviation from triplicate experiments. [c] Reference 30.

Generic alkyl halides fail to undergo alkylation with the bis-silylated pyrimidine intermediate, and base-mediated direct alkylation normally leads to a mixture of region isomers. As it turned out, the introduction of all-carbon chain into N-1 requires multiple protection and deprotection steps (Scheme 2D). In this event, the N-1 position was first protected with an easily introduced ethoxymethyl group, which allowed the protection of N-3 position with an acetophenone group. The N-1 ether linkage was then cleaved under acidic condition to yield the N-3 protected intermediate **35**. Base-mediated direct alkylation led to the incorporation of the carbon tethers followed by a Mg mediated N-3 deprotection to yield key N-1 alkylated intermediates **39**−**41**. All N-1 alkylated pyrimidine-2,4-diones were then oxidized with *m*-CPBA to produce desired N-3 hydroxylated compounds (Scheme 2).

Table 3. Effects of Hydrophobic Domain on IN Inhibition

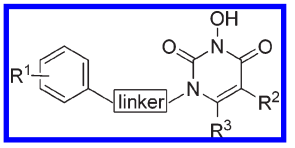

compd	R^1	linker	R^2	R^3	IN IC_{50} (μM)[a] 3′P	ST[b]
11[c]	H	CH_2OCH_2	*i*Pr	benzyl	>111	21 ± 2
51	H	CH_2OCH_2	*i*Pr	4-F-benzyl	>111	7.3 ± 0.8
52	F	CH_2OCH_2	*i*Pr	4-F-benzyl	>111	5.5 ± 0.7
53	H	CH_2OCH_2	Et	benzyl	>111	8.2 ± 1.0
54	H	CH_2OCH_2	Me	H	>111	75 ± 7
55	H	CH_2OCH_2	benzyl	Et	>111	36 ± 6
56	F	CH_2OCH_2	benzyl	Et	>111	11 ± 0.8
64	H	CH_2	*i*Pr	4-F-benzyl	>111	32 ± 6
65	F	CH_2	*i*Pr	4-F-benzyl	>111	73 ± 12
66	H	CH_2	*i*Pr	benzyl	>111	28 ± 2
67	H	CH_2	Et	benzyl	>111	>111
68	F	CH_2	Et	benzyl	>111	24 ± 3
69	H	CH_2	Me	H	>111	>111
70	F	CH_2	Me	H	>111	>111
75	H	CH_2	benzo (fused)		>111	>111
76	F	CH_2	benzo (fused)		>111	>111

[a] Concentration inhibiting enzymatic function by 50%. [b] Mean value ± standard deviation from triplicate experiments. [c] Reference 30.

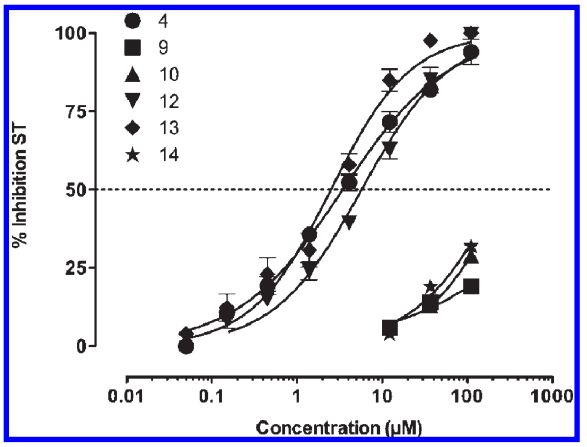

Figure 3. Dose response curves of compounds **4**, **9**−**10** and **12**−**14**.

The synthesis of hydrophobic domain with variable C-5 and C-6 substituents (Scheme 3A) was achieved through a similar N-3 hydroxylation of N-1 alkylated intermediates (**45**−**50** and **57**−**63**). Compounds with a slightly different scaffold, the 5, 6-benzopyrimidine-2,4-diones (**75**−**76**), were also prepared to probe the effect of a fused benzene ring on IN inhibition. These analogues were synthesized via a route depicted in Scheme 3C.

SAR on IN Inhibition. All synthetic analogues were first tested against recombinant HIV-1 IN using a gel assay. Both 3′P and ST functions were evaluated. As clearly shown in Tables 1−3, our scaffold tends to selectively inhibit ST as none of the analogues demonstrated inhibitory activity against 3′P.

Aromatic and Chelating Domains. We have shown previously[30] that removing the phenyl ring at the end of the N-1 pendant

dx.doi.org/10.1021/jm1014378 |*J. Med. Chem.* 2011, 54, 2282–2292

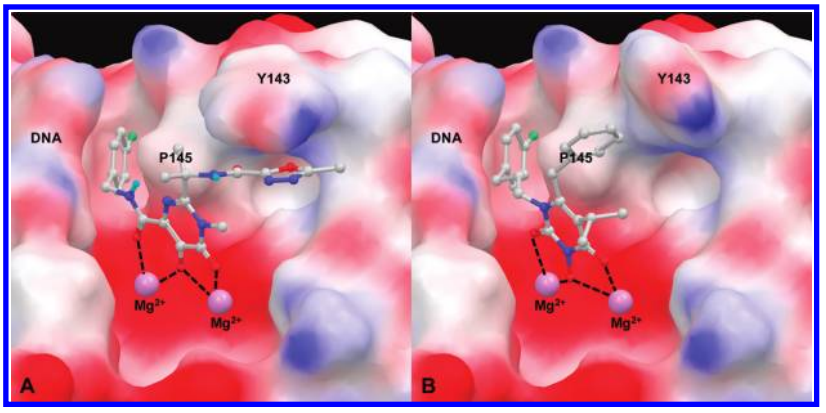

Figure 4. Docking of raltegravir (**1**, A) and inhibitor **43** (B) in HIV-1 IN CCD in complex with Mg^{2+} and DNA. The 3-N hydroxyl group simultaneously chelates to both Mg^{2+} ions while allowing the placement of the benzyl group into the protein−DNA interfacial hydrophobic pocket.

resulted in a significant loss of inhibition against IN and that without the OH group the N(3)H analogue is completely inactive against IN. These findings corroborate the pharmacophore hypothesis that HIV-1 IN inhibition requires minimally a chelating domain and an aromatic domain. In this study, additional analogues were synthesized to further study these two domains. As shown in Table 1 and Figure 3, halogen substitution of the N-1 benzyl seems to significantly benefit IN binding. A fluorination at the para position (inhibitor **4**) leads to a 6-fold improvement in IN inhibition over the unsubstituted compound **11**. Further improvement in activity was only marginal with a 3-chloro-2-fluoro substituted analogue **13**, whereas a 2,4-difluoro compound **12** showed slightly reduced inhibition when compared to **4** (Table 1). On the other hand, replacing the N-3 OH group with H, Me, OMe, or even NH_2 yielded compounds completely devoid of inhibitory activity against IN (**9**−**10** and **14**−**15**, Table 1), confirming the critical requirement of the N-3 OH for chelating Mg^{2+}. The lack of potency with the amino analogue **15** also reflects an inferior chelating ability of NH_2 for Mg^{2+} when compared to OH.[30]

The Linker Domain. Having established the chelating triad and the N-1 benzyl group as the two major structural determinants of our novel INI scaffold, our SAR efforts were then centered around the linker domain as it dictates the angle and distance between the chelator and benzyl group. Toward this end, we have designed linkers of different nature and length. Compounds **4** and **28**−**30** all have an ether linkage with incremental methylene groups (Table 2). Interestingly, these analogues all exhibited inhibitory activity in ST assay at low micromolar range, and demonstrated a discernible binding dependence on the length of the linker. As shown in Table 2, the 4-atom linker $(CH_2)_2OCH_2$ (inhibitor **28**) conferred the highest inhibition within this series and a reduced inhibition was achieved with compounds having a shorter (**4**) or longer linker (**29**−**30**). A similar albeit more sensitive trend was observed with compounds having an all carbon N-1 linker. In this case, short linkages, such as CH_2 (**32**) and $(CH_2)_2$ (**42**) appeared to pose severe binding difficulties while the 3- and 4-atom linkers $(CH_2)_3$ (**43**) and $(CH_2)_4$ (**44**) conferred a drastically improved inhibition against ST (Table 2). These findings strongly imply that the optimal IN inhibition entails a linker of 3−4 atoms. The nature of the linker (ether linkage vs all-carbon linkage) was also found to substantially impact IN inhibition as inhibitors **43** and **44** demonstrated significantly better inhibition than compound **28**. Detailed docking studies on the inhibitor binding may provide a molecular basis for this observation.

The Hydrophobic Domain. Synthetic analogues in these domains vary mainly in the size of the C-5 alkyl group (iPr, Et, and Me) and fluorine substitution on the C-6 benzyl. These changes impact most likely the steric hindrance and the overall hydrophobicity of these inhibitors. Interestingly, a C-5 ethyl group was found to confer significantly better inhibition than isopropyl group (**53** vs **11**, Table 3), indicating that less steric hindrance at C-5 could benefit IN binding. However, a reversed effect was observed in compounds with an N-1 linker of CH_2, wherein a C-5 ethyl substitution (**67**) caused a complete loss of inhibition when compared to a C-5 isopropyl substitution (**66**). On the other hand, swapping C5 and C6 substituents of inhibitor **53** seems to harm IN binding (**55** vs **53**) as the IC_{50} value increased by 4-fold. Notably, a *para*-fluoro substitution at the C-6 benzyl clearly favors IN inhibition (**53** vs **11**, **56** vs **55**). With a more dramatic change, a C-5 and C-6 fused benzene ring was found to render compounds **75**−**76** completely inactive against IN inhibition (Table 3). These findings indicate that the hydrophobic domain affects IN binding in a less comprehensible way and changes in this domain impact the activity most likely in concert with the linker domain.

Modeling. The common mode of inhibitory binding was explored through molecular docking using a homologous HIV IN model[38] constructed based on the crystal structure of prototype foamy virus (PFV) IN.[36] Significantly, the new inhibitor **43** fits perfectly into the IN binding site through two major binding domains also featured in raltegravir (**1**): the chelation of two Mg^{2+} ions and the placement of the 4-F-benzyl group into the protein−DNA interfacial hydrophobic pocket (Figure 4). The high degree of similarity shown between the binding of **1** and **43** confirms that our new molecular scaffold can effectively engage with HIV IN. Interestingly, while residue Y143 contributes siginificantly to binding of **1** through a π-stacking interaction (Figure 4A), the same interaction was not observed with our inhibitor **43** (Figure 4B), suggesting that our inhibitor could be less susceptible to resistance associated with Y143 mutation. It is also noteworthy that the linker domain is situated right in the hydrophobic cleft between residue P145 and viral DNA nucleobases. Therefore, an ether linkage may provide a less favorable hydrophobic interaction than an all-carbon linker, thus the observed reduced inhibition with the ether linkage (Table 2, **43** vs **28**).

Further validation was achieved by correlating the SAR of docked inhibitors **4**, **11**, **28**, **29**, **30**, **32**, **42**, **43**, **44**, and **66** as

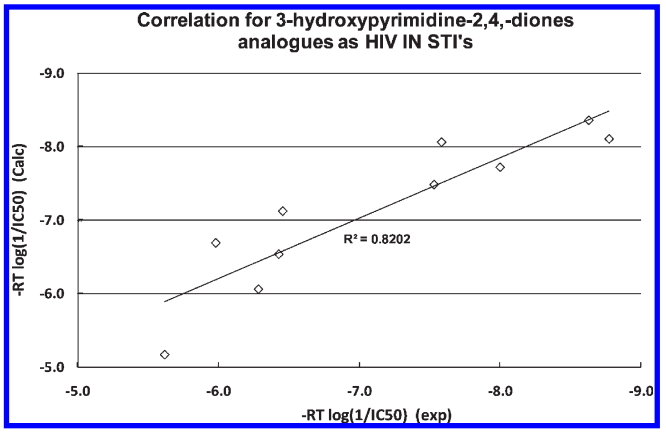

Figure 5. Strong correlation of docked 3-hydroxypyrimidine-2,4,-diones analogues supports a common mode of binding for HIV IN STI design.

Table 4. Anti-HIV-1 Activity of IN Inhibitors

	single concentration (10 μM)		dose response		
compd	CPE reduction (%)[a]	cell viability (%)	EC_{50} (μM)[b]	CC_{50} (μM)[c]	TI[d]
4[e]	100	100	0.024	>20	>833
11[e]	100	100	0.0080	>20	>2500
12	100	100	2.1	>100	>47
13	100	100	0.95	>100	>105
28	27	83	ND[f]	ND	
29	30	92	ND	ND	
30	12	88	ND	ND	
43	12	97	ND	ND	
44	6.0	94	ND	ND	
49	48	100	ND	ND	
50	10	92	ND	ND	
51	100	100	1.1	>20	>18

[a] Reduction of viral cytopathic effect, indicating inhibitory activity of a compound. [b] Concentration inhibiting virus replication by 50%. [c] Concentration resulting in 50% cell death. [d] Therapeutic index, defined by CC_{50}/EC_{50}. [e] Reference 30. [f] Not determined.

shown in Figure 5. The outstanding correlation observed between these two sets of IC_{50} data (expt vs calcd, correlation coefficiency = 0.82) supports our docking model with a common mode of binding as a valid platform for HIV IN inhibitor design.

Antiviral Assay. To evaluate the antiviral activity of newly synthesized INIs, all compounds with an IC_{50} of 10 μM or lower from IN ST assay were tested against HIV-1IIIB in CEM-SS cells using an assay based on viral cytopathic effect (CPE). In this assay, the reduction of CPE was used to indicate the antiviral activity of a compound. All selected compounds were first screened under a single concentration (10 μM). Inhibitors with excellent CPE reduction and cell viability from this screening assay were further tested in a dose response fashion, from which the EC_{50} and CC_{50} were determined. Table 4 summarizes the antiviral testing results.

Remarkably, compounds **43** and **44**, the two most potent INIs from IN ST assay with submicromolar IC_{50}s, have shown only marginal activity against HIV-1 at 10 μM (Table 4). This finding strongly suggests that despite their ability to confer exceptional

Table 5. Fold Resistance of Inhibitors 4 and 13 against IN Mutants

	fold resistance[a,b]		
IN mutants	**4**[c]	**13**	**1**
G140S/Q148H	10/13	14/17	148/139
Y143R	7/4	7/5	24/28
N155H	5/6	5/7	10/8

[a] Fold resistance is defined by $IC_{50(mutant)}/IC_{50(WT)}$. [b] Values from two independent experiments. [c] Reference 30.

Table 6. Fold Resistance of Inhibitors 4 and 13 against Raltegravir-Resistant HIV-1 Strains

		fold resistance[a]		
viruses	major mutations	**4**[b]	**13**[c]	**1**
8070−2	G140S/Q148H	7.3	>2.0	>855
1556−1	Y143C	5.9	>1.7	>855
4736−2	N155H	3.1	>5.1	149

[a] Fold resistance is defined by $EC_{50(mutant)}/EC_{50(WT)}$. [b] Reference 30. [c] Toxicity observed (TC_{50} = 2.0 μM).

IN inhibition in biochemical assays, all-carbon linkers lack the proper physicochemical properties for the compounds to reach their target in cell culture. By contrast, with the exception of compounds having a *para*-fluorine at the C-6 benzyl group (**49**−**50**, Table 4), INIs with an ether linkage of CH_2OCH_2 (**4**, **11**−**13**, and **51**) showed antiviral activity at the low micromolar to low nanomolar range without appreciable cytotoxicity (Table 4). Longer ether linkages that produced excellent anti-IN activity for compounds **28**−**30** did not generate similar activity in the antiviral assay, further demonstrating that additional CH_2s in the linker domain hinder antiviral activity.

Resistance. To establish the resistance profile of our inhibitors, we first tested two representative inhibitors **4** and **13** against HIV IN mutants. In this study, major mutants associated with raltegravir resistance,[23,24] namely a G140S/Q148H double mutant and two single mutants Y143R and N155H were employed. The results are summarized in Table 5. Notably, the G140S/Q148H double mutant which causes high resistance to raltegravir (**1**) yielded a much lower fold resistance to **4** and **13**, whereas the two single mutants confer comparable resistance to **4**, **13** and **1**, suggesting a potentially common binding mode for these inhibitors.

On the basis of these biochemical data, inhibitors **4** and **13** were further evaluated in cell culture against raltegravir-resistant HIV strains. Unlike the initial antiviral assay wherein HIV-1 IIIB was used in CEM-SS cells, the resistance studies were carried out with NL4−3 based viral strains in MT-4 cells. Selected strains contain major mutations corresponding to the IN mutants (Table 6 vs Table 5). As shown in Table 6, all three viral strains show a high level resistance to raltegravir (**1**). Interestingly, although likely within experimental variations, the small fold-resistances observed with inhibitor **4** (Table 6) correlate closely with resistance observed with IN mutants in biochemical assays (Table 5). The testing of inhibitor **13** was complicated by its

dx.doi.org/10.1021/jm1014378 |*J. Med. Chem.* 2011, 54, 2282–2292

toxicity observed in MT-4 cells. Notably the same compound did not show toxicity in CEM-SS cells ($TC_{50} > 100\ \mu M$, Table 4). On the other hand, antiviral assay with two HIV-1_{NL4-3} strains containing major mutations associated with NNRTI resistance, K103N or Y181C, revealed a fold-resistance of 16 and 48, respectively, to inhibitor **4**.[46] These results suggest that the overall antiviral activity of **4** could reflect a concerted yet not necessarily balanced inhibition to both RT and IN.

CONCLUSION

Through complete SAR and docking studies we have demonstrated that the N-3 OH group and the 4-F-benzyl moiety on the N-1 side chain are the key structural determinants for IN inhibition, and that the linker domain sits in a hydrophobic cleft between DNA nucleobases and P145. Therefore, both the nature and the length of the linker greatly impact IN binding, with the optimal IN inhibition entailing a 3−4 atom all-carbon linkage. However, studies in cell culture revealed that inhibitors with an all-carbon linker generally lack antiviral activity, presumably due to unfavored physicochemical properties. Resistance studies with raltegravir-resistant IN mutants as well as HIV-1_{NL4-3} viral strains demonstrated low level resistances toward inhibitors **13** and **4**, likely due to their anti-RT activity. In the end, compounds (**4**, **11**, and **13**) featuring a CH_2OCH_2 linker demonstrate low micromolar IN inhibition and nanomolar anti-HIV activity, and are suitable for further development.

EXPERIMENTAL SECTION

Chemistry. *General Procedures.* All commercial chemicals were used as supplied unless otherwise indicated. Dry solvents (THF, Et_2O, CH_2Cl_2, and DMF) were dispensed under argon from an anhydrous solvent system with two packed columns of neutral alumina or molecular sieves. Flash chromatography was performed on a Teledyne Combiflash RF-200 with RediSep columns (silica) and indicated mobile phase. All reactions were performed under inert atmosphere of ultrapure argon with oven-dried glassware. ^1H and ^{13}C NMR spectra were recorded on a Varian 600 MHz spectrometer. Mass data were acquired on an Agilent TOF II TOS/MS spectrometer capable of ESI and APCI ion sources. Analysis of sample purity was performed on a Varian Prepstar SD-1 HPLC system with a Varian Microsorb-MW 100−5 C18 column (250 mm × 4.6 mm): solvent A = H_2O, solvent B = MeCN; flow rate = 1.0 mL/min; method: linear 30−95% (B) over 25 min. All tested compounds have a purity ≥96%.

*6-Benzyl-1-(benzyloxymethyl)-5-isopropylpyrimidine-2,4(1H,3H)-dione (**6**).*[44] To a suspension of paraformaldehyde (144 mg, 4.80 mmol) in TMSCl (2.0 mL) was added benzyl alcohol (518 mg, 4.80 mmol) at room temperature. The reaction mixture was stirred until a clear solution was formed. The solution was concentrated under reduced pressure to give benzyl chloromethyl ether as oil, which was taken to the next step without further purification. To a suspension of pyrimidine **5** (976 mg 4.00 mmol) in 16 mL of anhydrous DCM was added BSA (2.16 mL, 8.80 mmol) at room temperature. The resulting mixture was stirred until a clear solution was achieved. The freshly prepared benzyl chloromethy ether was added to this solution followed by the addition of a catalytic amount of TBAI. The reaction mixture was kept overnight and then quenched by adding a saturated aqueous solution of $NaHCO_3$. The aqueous phase was extracted with CH_2Cl_2 (20 mL × 3). The combined organic extracts were dried over Na_2SO_4 and concentrated under reduced pressure. The resultant residue was subjected to combiflash (Hex/EtOAc, 2:1) to afford compound **6** (1.25 g, 86%) as a white solid. ^1H NMR (600 MHz, $CDCl_3$) δ 7.28 (m, 6H), 7.20 (m, 2H), 7.00 (d, J = 7.8 Hz, 2H), 5.14 (s, 2H), 4.59 (s, 2H), 4.10 (s, 2H), 2.79 (septet, J = 6.6 Hz, 1H), 1.21 (d, J = 6.6 Hz, 6H). MS (ESI+) m/z: 365.17 (M + 1).

*6-Benzyl-1-((2,4-difluorobenzyloxy)methyl)-5-isopropylpyrimidine-2,4(1H,3H)-dione (**7**).* This compound was prepared as a white solid following the procedure described for the preparation of **6**; yield 88%. ^1H NMR (600 MHz, $CDCl_3$) δ 9.32 (s, 1H), 7.34 (m, 3H), 7.26 (t, J = 7.8 Hz, 1H), 7.07 (d, J = 7.8 Hz, 2H), 6.86 (t, J = 9.0 Hz, 1H), 6.81 (d, J = 9.0 Hz, 1H), 5.20 (s, 2H), 4.64 (s, 2H), 4.16 (s, 2H), 2.87 (m, 1H), 1.28 (d, J = 6.6 Hz, 6H). MS (ESI−) m/z: 399.42 (M − 1).

*6-Benzyl-1-((3-chloro-2-fluorobenzyloxy)methyl)-5-isopropylpyrimidine-2,4(1H,3H)-dione (**8**).* This compound was prepared as a white solid following the procedure described for the preparation of **6**; yield 90%. ^1H NMR (600 MHz, $CDCl_3$) δ 8.96 (b, 1H), 7.36 (m, 3H), 7.33 (t, J = 7.8 Hz, 2H), 7.10 (m, 3H), 5.21 (s, 2H), 4.69 (s, 2H), 4.16 (s, 2H), 2.87 (m, 1H), 1.28 (d, J = 6.6 Hz, 6H). MS (ESI−) m/z: 415.87 (M − 1).

*6-Benzyl-1-((4-fluorobenzyloxy)methyl)-5-isopropylpyrimidine-2,4(1H,3H)-dione (**9**).* This compound was prepared as a white solid following the procedure described for the preparation of **6**; yield 89%. ^1H NMR (600 MHz, $CDCl_3$) δ 8.97 (b, 1H), 7.34 (t, J = 7.2 Hz, 2H), 7.30 (m, 3H), 7.07 (d, J = 7.8 Hz, 2H), 7.03 (m, 2H), 5.20 (s, 2H), 4.61 (s, 2H), 4.16 (s, 2H), 2.88 (septet, J = 7.2 Hz, 1H), 1.28 (d, J = 7.2 Hz, 6H). MS (ESI+) m/z: 383.18 (M + 1).

*6-Benzyl-1-((4-fluorophenethoxy)methyl)-5-isopropylpyrimidine-2,4(1H,3H)-dione (**25**).* This compound was prepared as a white solid following the procedure described for the preparation of **6**; yield 89%. ^1H NMR (600 MHz, $CDCl_3$) δ 8.89 (b, 1H), 7.27 (t, J = 7.2 Hz, 2H), 7.20 (m, 1H), 7.08(m, 2H), 6.99 (d, J = 7.8 Hz, 2H), 6.91 (t, J = 8.4 Hz, 2H), 5.04 (s, 2H), 3.94 (s, 2H), 3.71 (t, J = 6.6 Hz, 2H), 2.74 (m, 3H), 1.20 (d, J = 6.6 Hz, 6H). MS (ESI−) m/z: 395.45 (M − 1).

*6-Benzyl-1-((3-(4-fluorophenyl)propoxy)methyl)-5-isopropylpyrimidine-2,4(1H,3H)-dione (**26**).* This compound was prepared as a white solid following the procedure described for the preparation of **6**; yield 83%. ^1H NMR (600 MHz, $CDCl_3$) δ 8.97 (b, 1H), 7.29 (t, J = 7.8 Hz, 2H), 7.21 (t, J = 7.8 Hz, 1H), 7.05 (m, 4H), 6.89 (t, J = 9.0 Hz, 2H), 5.05 (s, 2H), 4.11 (s, 2H), 3.50 (t, J = 6.0 Hz, 2H), 2.87 (septet, J = 7.2 Hz, 1H), 2.56 (t, J = 7.8 Hz, 2H), 1.78 (m, 2H), 1.23 (d, J = 6.6 Hz, 6H). MS (ESI−) m/z: 409 (M − 1).

*6-Benzyl-1-((4-(4-fluorophenyl)butoxy)methyl)-5-isopropylpyrimidine-2,4(1H,3H)-dione (**27**).* This compound was prepared as a white solid following the procedure described for the preparation of **6**; yield 84%. ^1H NMR (600 MHz, $CDCl_3$) δ 10.01 (b, 1H), 7.34 (t, J = 7.8 Hz, 2H), 7.26 (t, J = 7.2 Hz, 1H), 7.10 (m, 4H), 6.94 (d, J = 9.0 Hz, 2H), 5.23 (s, 2H), 4.16 (s, 2H), 3.58 (t, J = 6.6 Hz, 2H), 2.86 (septet, J = 7.2 Hz, 1H), 2.58 (t, J = 7.2 Hz, 2H), 1.63 (m, 2H), 1.56 (m, 2H), 1.27 (d, J = 7.2 Hz, 6H). MS (ESI−) m/z: 423.51 (M − 1).

*6-Benzyl-1-(ethoxymethyl)-5-isopropylpyrimidine-2,4(1H,3H)-dione (**33**).* This compound was prepared as a white solid following the procedure described for the preparation of **6**; yield 89%. ^1H NMR (600 MHz, $CDCl_3$) δ 8.68 (b, 1H), 7.29 (t, J = 7.8 Hz, 2 H), 7.22 (m, 2H), 7.06 (d, J = 7.8 Hz, 1H), 5.05 (s, 2H), 4.11 (s, 2H), 3.56 (q, J = 7.2 Hz, 2H), 2.81 (septet, J = 7.2 Hz, 1H), 1.22 (d, J = 6.6 Hz, 6H), 1.11 (t, J = 7.2 Hz, 3H); MS (ESI−) m/z: 301.37 (M − 1).

*1-(Benzyloxymethyl)-5-methylpyrimidine-2,4(1H,3H)-dione (**48**).* This compound was prepared as a white solid following the procedure described for the preparation of **6**; yield 82%. ^1H NMR (600 MHz, $CDCl_3$) δ 9.21 (b, 1H), 7.34 (m, 5H), 7.10 (s, 1H), 5.21 (s, 2H), 4.66 (s, 2H), 4.62 (s, 2H), 1.91 (s, 3H). MS (ESI−) m/z: 245.10 (M − 1).

*5-Benzyl-1-(benzyloxymethyl)-6-ethylpyrimidine-2,4(1H,3H)-dione (**49**).* This compound was prepared as a white solid following the procedure described for the preparation of **6**; yield 78%. ^1H NMR (600 MHz, $CDCl_3$) δ 9.64 (s, 1H), 7.31 (m, 4H), 7.24 (m, 3H), 6.99 (m, 3H), 5.43 (s, 2H), 4.67 (s, 2H), 4.08 (s, 2H), 2.73 (q, J = 6.6 Hz, 2H), 1.06 (t, J = 6.6 Hz, 3H). MS (ESI−) m/z: 349.62 (M − 1).

*5-Benzyl-6-ethyl-1-((4-fluorobenzyloxy)methyl)pyrimidine-2,4(1H,3H)-dione (**50**).* This compound was prepared as a white solid following the procedure described for the preparation of **6**; yield 80%. ^{1}H NMR (600 MHz, $CDCl_3$) δ 9.51 (s, 1H), 7.29 (t, J = 7.2 Hz, 4H), 7.20 (d, J = 6.6 Hz, 2H), 7.00 (t, J = 6.6 Hz, 2H), 5.41 (s, 2H), 4.62 (s, 2H), 4.08 (s, 2H), 2.72 (q, J = 6.6 Hz, 2H), 1.07 (t, J = 6.6 Hz, 3H). MS (ESI−) m/z: 367.15 (M − 1).

*6-Benzyl-1-((4-fluorobenzyloxy)methyl)-5-isopropyl-3-methylpyrimidine-2,4(1H,3H)-dione (**10**).* A mixture of compound **9** (60 mg, 0.16 mmol), methyl iodide (27 mg, 0.19 mmol), and Cs_2CO_3 (61 mg, 0.19 mmol) in 2 mL of THF was stirred under 40 °C for 3 h and then allowed to cool to room temperature. The reaction mixture was quenched by adding 5 mL of H_2O and extracted with EtOAc (10 mL × 3). The combined organic phases were dried over Na_2SO_4 and then concentrated under reduced pressure. The resultant residue was purified with Combiflash to give compound **10** (40 mg, 63%) as clean oil. ^{1}H NMR (600 MHz, $CDCl_3$) δ 7.25 (t, J = 7.8 Hz, 2H), 7.21 (m, 3H), 6.99 (d, J = 7.2 Hz, 2H), 6.95 (t, J = 8.4 Hz, 2H), 5.16 (s, 2H), 4.53 (s, 2H), 4.09 (s, 2H), 3.28 (s, 3H), 2.87 (septet, J = 7.2 Hz, 1H), 1.22 (d, J = 7.2 Hz, 6H). ^{13}C NMR (150 MHz, $CDCl_3$) δ 163.2, 161.8, 161.5, 152.6, 146.0, 135.4, 133.2 (d, J = 3.3 Hz), 129.6 (d, J = 7.8 Hz), 129.2, 127.3 (d, J = 7.4 Hz), 118.9, 115.4 (d, J = 21.2 Hz), 73.7, 71.0, 33.4, 28.2, 27.9, 20.4. MS (ESI−) m/z: 395.45 (M − 1).

*6-Benzyl-1-((4-fluorobenzyloxy)methyl)-5-isopropyl-3-methoxypyrimidine-2,4(1H,3H)-dione (**14**).* This compound was prepared following the procedure described for the preparation of **10**; yield 53%. ^{1}H NMR (600 MHz, $CDCl_3$) δ 7.27 (t, J = 8.4 Hz, 2H), 7.24 (m, 3H), 6.99 (d, J = 7.2 Hz, 2H), 6.96 (t, J = 8.4 Hz, 2H), 5.14 (s, 2H), 4.55 (s, 2H), 4.08 (s, 2H), 3.94 (s, 3H), 2.85 (septet, J = 7.2 Hz, 1H), 1.22 (d, J = 7.2 Hz, 6H). MS (ESI−) m/z: 411.45 (M − 1).

*3-Amino-6-benzyl-1-(benzyloxymethyl)-5-isopropylpyrimidine-2,4(1H,3H)-dione (**15**).*[30] To a solution of **6** (60 mg, 0.16 mmol) in l.0 mL of THF was added NaH (31 mg, 0.82 mmol) at 0 °C. This reaction mixture was allowed to warm to room temperature over 1 h and then cooled to 0 °C followed by the addition of *O*-(mesitylsulfonyl)hydroxylamine[47] (MSH, 66 mg, 0.32 mmol). After stirring for 0.5 h, this reaction mixture was stirred at rt overnight. The reaction was quenched by adding 10 mL of H_2O; the aqueous phase was then extracted with ethyl acetate (10 mL × 3). The combined organic extracts were dried over Na_2SO_4 and concentrated under reduced pressure. The resultant residue was subjected to Combiflash (Hex/EtOAc, 1:1) to give compound **15** (22 mg, 54% based on consumed start material) as a white solid. ^{1}H NMR (600 MHz, $CDCl_3$) δ 7.33−7.26 (m, 8H), 7.04−7.03 (d, J = 7.2 Hz, 2H), 5.24 (s, 2H), 4.66 (s, 2H), 4.19 (s, 2H), 2.90 (septet, J = 7.2 Hz, 1H), 1.29 (d, J = 6.6 Hz, 6H). HRMS (ESI−) calcd for $C_{22}H_{25}N_3O_3$ $[M - H]^-$ 380.1969, found 380.1976 (E = −1.9 ppm).

*6-Benzyl-1-((4-fluorobenzyloxy)methyl)-3-hydroxy-5-isopropylpyrimidine-2,4(1H,3H)-dione (**4**).*[47] To a solution of **9** (100 mg, 0.26 mmol) in 6 mL of THF was added NaH (31 mg, 1.30 mmol) at 0 °C. This reaction mixture was allowed to warm to room temperature over 1 h and then cooled to 0 °C followed by the addition of *m*-CPBA (135 mg, 0.79 mmol). This reaction mixture was allowed to warm to room temperature and stirred overnight. After the reaction was quenched by adding 10 mL of H_2O, the aqueous phase was acidified with 1N HCl to pH = 7 and then extracted with ethyl acetate (10 mL × 3). The combined organic extracts were dried over Na_2SO_4 and concentrated under reduced pressure. The resultant residue was subjected to Combiflash (Hex/EtOAc, 1:1) to give compound **4** (38 mg, 72% based on consumed start material) as a white solid. ^{1}H NMR (600 MHz, $CDCl_3$) δ 7.33−7.26 (m, 5H), 7.04−6.99 (m, 4H), 5.03 (s, 2H), 4.64 (s, 2H), 4.19 (s, 2H), 2.90 (septet, J = 7.2 Hz, 1H), 1.29 (d, J = 6.6 Hz, 6H). ^{13}C NMR (150 MHz, $CDCl_3$) δ 163.3, 162.4, 161.6, 152.1, 148.3, 135.2, 133.1(d, J = 3.3 Hz), 129.7 (d, J = 7.8 Hz), 129.2, 127.2 (d, J = 6.8 Hz), 119.9, 115.4 (dd, J = 21.2 Hz), 72.8, 70.9, 33.5, 28.2, 20.4. HRMS (ESI−) calcd for $C_{22}H_{23}FN_2O_4$ $[M - H]^-$ 399.1715, found 399.1705 (E = 2.4 ppm).

*6-Benzyl-1-(benzyloxymethyl)-3-hydroxy-5-isopropylpyrimidine-2,4(1H,3H)-dione (**11**).* This compound was prepared as a white solid following the procedure described for the preparation of **4**; yield 53%. ^{1}H NMR (600 MHz, $CDCl_3$) δ 7.32−7.30 (m, 7H), 7.02 (J = 7.2 Hz, 2H), 5.30 (s, 2H), 4.67 (s, 2H), 4.19 (s, 2H), 2.90 (septet, J = 7.2 Hz, 1H), 1.28 (d, J = 6.6 Hz, 6H). ^{13}C NMR (150 MHz, $CDCl_3$) δ 162.2, 151.9, 148.4, 137.3, 135.3, 129.1, 128.5, 128.0, 127.8, 127.3, 127.2, 119.8, 73.0, 71.8, 33.5, 28.2, 20.4. HRMS (ESI−) calcd for $C_{22}H_{24}N_2O_4$ $[M - H]^-$ 381.1809, found 381.1803 (E = 1.5 ppm).

*6-Benzyl-1-((2,4-difluorobenzyloxy)methyl)-3-hydroxy-5-isopropylpyrimidine-2,4(1H,3H)-dione (**12**).* This compound was prepared as a white solid following the procedure described for the preparation of **4**; yield 73%. ^{1}H NMR (600 MHz, $CDCl_3$) δ 7.18 (m, 1H). 7.20 (m, 2H), 7.14 (t, J = 7.2 Hz, 1H), 6.97 (d, J = 7.8 Hz, 2H), 6.73 (td, J = 1.8, 9.6 Hz, 1H), 6.67 (td, J = 1.8, 9.6 Hz, 1H), 5.13 (s, 2H), 4.55 (s, 2H), 4.04 (s, 2H), 2.75 (m, 1H), 1.13 (d, J = 6.6 Hz, 6H). ^{13}C NMR (150, $CDCl_3$) δ 163.8 (d, J = 11.7 Hz), 162.1(dd, J = 7.8, 19.5 Hz), 160.4 (d, J = 11.7 Hz), 148.3, 135.2, 131.5 (d, J = 7.8 Hz), 129.2, 127.2, 120.4 (d, J = 15.6 Hz), 120.0, 111.2 (dd, J = 3.9, 21.2 Hz), 104.1 (t, J = 25.2 Hz), 72.7, 64.9, 33.4, 28.3, 20.3. HRMS (ESI−) calcd for $C_{22}H_{22}F_2N_2O_4$ $[M - H]^-$ 415.1475, found 415.1473 (E = 0.45 ppm).

*6-Benzyl-1-((3-chloro-2-fluorobenzyloxy)methyl)-3-hydroxy-5-isopropylpyrimidine-2,4(1H,3H)-dione (**13**).* This compound was prepared as a white solid following the procedure described for the preparation of **4**; yield 85%. ^{1}H NMR (600 MHz, CD_3OD) δ 7.32 (t, J = 6.6 Hz, 1H), 7.23 (m, 3H), 7.18 (t, J = 7.2 Hz, 1H), 7.05 (t, J = 7.8 Hz, 1H), 7.00 (d, J = 7.8 Hz, 2H), 5.29 (s, 2H), 4.67 (s, 2H), 4.11 (s, 2H), 2.87 (m, 1H), 1.22 (d, J = 7.2 Hz, 6H). ^{13}C NMR (150, $CDCl_3$) 163.7 (d, J = 11.7 Hz), 162.1 (t, J = 11.7 Hz), 160.4 (t, J = 11.7 Hz), 159.7, 144.2, 135.5, 131.8 (d, J = 11.7 Hz), 129.1, 127.3(t, J = 16.2 Hz), 120.5 (d, J = 11.1 Hz), 118.2, 116.6, 111.1 (dd, J = 3.5, 21.3 Hz), 103.9 (t, J = 25.1 Hz), 72.9, 65.5, 33.4, 28.3, 20.4. HRMS (ESI−) calcd for $C_{22}H_{22}ClFN_2O_4$ $[M - H]^-$ 431.1179, found 431.1181 (E = −0.83 ppm).

*6-Benzyl-1-((4-fluorophenethoxy)methyl)-3-hydroxy-5-isopropylpyrimidine-2,4(1H,3H)-dione (**28**).* This compound was prepared as a white solid following the procedure described for the preparation of **4**; yield 66%. ^{1}H NMR (600 MHz, $CDCl_3$) δ 7.34 (t, J = 7.2 Hz, 2H), 7.29 (d, J = 7.2 Hz, 1H), 7.14 (m, 2H), 7.03 (d, J = 7.8 Hz, 2H), 6.97 (t, J = 8.4 Hz, 2H), 5.19 (s, 2H), 4.04 (s, 2H), 3.82 (t, J = 6.6 Hz, 2H), 2.88 (septet, J = 7.2 Hz, 1H), 2.81 (t, J = 6.6 Hz, 2H), 1.28 (d, J = 6.6 Hz, 6H). ^{13}C NMR (150 MHz, $CDCl_3$) δ 162.5 (d, J = 16.2 Hz), 160.7, 155.5, 152.1, 148.4, 135.4, 134.2 (d, J = 2.9 Hz), 130.3 (d, J = 7.8 Hz), 129.2, 127.2, 119.8, 115.2 (d, J = 21.2 Hz), 72.9, 70.0, 35.1, 33.3, 28.2, 20.4. HRMS (ESI+) calcd for $C_{23}H_{25}FN_2O_4$ $[M + H]^+$ 413.1871, found 413.1868 (E = 0.76 ppm).

*6-Benzyl-1-((3-(4-fluorophenyl)propoxy)methyl)-3-hydroxy-5-isopropylpyrimidine-2,4(1H,3H)-dione (**29**).* This compound was prepared as a white solid following the procedure described for the preparation of **4**; yield 71%. ^{1}H NMR (600 MHz, $CDCl_3$) δ 7.33 (m, 2H), 7.26 (m, 1H), 7.07 (m, 2H), 7.01 (m, 2H), 6.95 (m, 2H), 5.19 (s, 2H), 4.18 (s, 2H), 3.58 (m, 2H), 2.89 (septet, J = 7.2 Hz, 1H), 2.60 (m, 2H), 1.82 (m, 2H), 1.29 (d, J = 6.6 Hz, 6H). ^{13}C NMR (150 MHz, $CDCl_3$) δ 162.9, 162.1, 160.5, 152.4, 148.5, 137.2 (d, J = 3.3 Hz), 135.4, 129.7 (d, J = 7.8 Hz), 129.2, 127.3 (d, J = 7.8 Hz), 119.9, 115.2 (d, J = 20.6 Hz), 73.0, 68.4, 33.5, 31.3, 31.1, 28.2, 20.4. HRMS (ESI+) calcd for $C_{24}H_{27}FN_2O_4$ $[M + H]^+$ 427.2028, found 427.2026 (E = 0.38 ppm).

*6-Benzyl-1-((4-(4-fluorophenyl)butoxy)methyl)-3-hydroxy-5-isopropylpyrimidine-2,4(1H,3H)-dione (**30**).* This compound was prepared as a white solid following the procedure described for the preparation of **4**; yield 64%. ^{1}H NMR (600 MHz, $CDCl_3$) δ 7.34 (t, J = 7.2 Hz, 2H), 7.28 (d, J = 7.2 Hz, 1H), 7.11 (dd, J = 1.8, 7.8 Hz, 2H), 7.07 (d, J = 7.8 Hz, 2H), 6.96 (t, J = 8.4 Hz, 2H), 5.21 (s, 2H), 4.19 (s, 2H), 3.60 (t, J = 6.0

Hz, 2H), 2.91 (septet, J = 7.2 Hz, 1H), 2.58 (t, J = 7.2 Hz, 2H), 1.63 (m, 2H), 1.58 (m, 2H), 1.29 (d, J = 6.6 Hz, 6H). ^{13}C NMR (150, $CDCl_3$) δ 162.7, 162.0, 160.4, 152.2, 148.5, 137.8 (d, J = 3.3 Hz), 135.4, 129.7 (d, J = 7.8 Hz), 129.2, 127.3 (d, J = 7.8 Hz), 119.8, 115.0 (d, J = 20.7 Hz), 73.1, 69.3, 34.7, 33.4, 29.2, 28.9, 28.1, 20.3. HRMS (ESI+) calcd for $C_{25}H_{29}FN_2O_4$ $[M + H]^+$ 441.2184, found 441.2164 (E = 4.6 ppm).

*6-Benzyl-1-(4-fluorobenzyl)-3-hydroxy-5-isopropylpyrimidine-2,4(1H,3H)-dione (**32**).* This compound was prepared as a white solid following the procedure described for the preparation of **4**; yield 72%. ^{1}H NMR (600 MHz, $CDCl_3$) δ 7.30 (t, J = 7.2 Hz, 2H), 7.05−7.03 (m, 3H), 6.98 (d, J = 7.2 Hz, 2H), 6.94 (m, 2H), 4.88 (s, 2H), 3.83 (s, 2H), 2.81 (septet, J = 7.2 Hz, 1H), 1.22 (d, J = 6.6 Hz, 6H). HRMS (ESI+) calcd for $C_{21}H_{21}FN_2O_3$ $[M + H]^+$ 369.1609, found 369.1608 (E = 0.26 ppm).

*6-Benzyl-1-(4-fluorophenethyl)-3-hydroxy-5-isopropylpyrimidine-2,4(1H,3H)-dione (**42**).* This compound was prepared as a white solid following the procedure described for the preparation of **4**; yield 62%. ^{1}H NMR (600 MHz, $CDCl_3$) δ 7.26−7.24 (m, 2H), 7.21 (m, 1H), 6.97 (m, 2H), 6.89−6.88 (m, 2H), 6.85−6.84 (m, 2H), 3.79 (s, 2H), 3.73 (t, J = 7.8 Hz, 2H), 2.82 (septet, J = 7.2 Hz, 1H), 2.68 (t, J = 7.8 Hz, 2H), 1.29 (d, J = 6.6 Hz, 6H). HRMS (ESI+) calcd for $C_{23}H_{23}FN_2O_3$ $[M + H]^+$ 383.1765, found 383.1768 (E = 0.38 ppm).

*6-Benzyl-1-(3-(4-fluorophenyl)propyl)-3-hydroxy-5-isopropylpyrimidine-2,4(1H,3H)-dione (**43**).* This compound was prepared as a white solid following the procedure described for the preparation of **4**; yield 72%. ^{1}H NMR (600 MHz, $CDCl_3$) δ 7.21 (m, 3H), 6.94 (m, 2H), 6.87 (t, J = 8.4 Hz, 2H), 6.75 (d, J = 7.8 Hz, 2H), 3.71 (s, 2H), 3.58 (t, J = 7.2 Hz, 2H), 2.78 (septet, J = 7.2 Hz, 1H), 2.46 (t, J = 7.2 Hz, 2H), 1.79 (m, 2H), 1.29 (d, J = 6.6 Hz, 6H). HRMS (ESI+) calcd for $C_{23}H_{25}FN_2O_3$ $[M + H]^+$ 397.1922, found 397.1924 (E = −0.51 ppm).

*6-Benzyl-1-(4-(4-fluorophenyl)butyl)-3-hydroxy-5-isopropylpyrimidine-2,4(1H,3H)-dione (**44**).* This compound was prepared as a white solid following the procedure described for the preparation of **4**; yield 65%. ^{1}H NMR (600 MHz, $CDCl_3$) δ 7.34 (t, J = 7.2 Hz, 2H), 7.28 (d, J = 7.8 Hz, 1H), 7.05 (m, 4H), 6.94 (t, J = 8.4 Hz, 2H), 3.92 (s, 2H), 3.73 (m, 2H), 2.87 (septet, J = 7.2 Hz, 1H), 2.51 (t, J = 7.2 Hz, 2H), 1.56 (m, 2H), 1.51 (m, 2H), 1.27 (d, J = 7.2 Hz, 6H). HRMS (ESI+) calcd for $C_{24}H_{27}FN_2O_3$ $[M + H]^+$ 411.2078, found 411.2081 (E = −0.62 ppm).

*1-(Benzyloxymethyl)-6-(4-fluorobenzyl)-3-hydroxy-5-isopropylpyrimidine-2,4(1H,3H)-dione (**51**).* This compound was prepared as a white solid following the procedure described for the preparation of **4**; yield 74%. ^{1}H NMR (600 MHz, $CDCl_3$) δ 7.32−7.27 (m, 5H), 7.00−6.98 (m, 4H), 5.28 (s, 2H), 4.67 (s, 2H), 4.14 (s, 2H), 2.81 (septet, J = 7.2 Hz, 1H), 1.27 (d, J = 6.6 Hz, 6H). HRMS (ESI−) calcd for $C_{22}H_{23}FN_2O_4$ $[M - H]^-$ 399.1715, found 399.1706 (E = 2.1 ppm).

*6-(4-Fluorobenzyl)-1-((4-fluorobenzyloxy)methyl)-3-hydroxy-5-isopropylpyrimidine-2,4(1H,3H)-dione (**52**).* This compound was prepared as a white solid following the procedure described for the preparation of **4**; yield 72%. ^{1}H NMR (600 MHz, $CDCl_3$) δ 7.28−7.27 (m, 6H), 7.00 (d, J = 7.2 Hz, 2H), 5.24 (s, 2H), 4.61 (s, 2H), 4.12 (s, 2H), 2.83 (septet, J = 7.2 Hz, 1H), 1.25 (d, J = 6.6 Hz, 6H). HRMS (ESI−) calcd for $C_{22}H_{22}F_2N_2O_4$ $[M - H]^-$ 417.1620, found 417.1620 (E = 0.10 ppm).

*6-Benzyl-1-(benzyloxymethyl)-5-ethyl-3-hydroxypyrimidine-2,4(1H,3H)-dione (**53**).* This compound was prepared as a white solid following the procedure described for the preparation of **4**; yield 70%. ^{1}H NMR (600 MHz, $CDCl_3$) δ 7.33−7.27 (m, 8H), 7.03 (d, J = 7.8 Hz, 2H), 5.26 (s, 2H), 4.65 (s, 2H), 4.15 (s, 2H), 2.51 (q, J = 7.8 Hz, 2H), 1.06 (t, J = 7.2 Hz, 3H). HRMS (ESI−) calcd for $C_{21}H_{22}N_2O_4$ $[M - H]^-$ 367.1652, found 367.1641 (E = 3.1 ppm).

*1-(Benzyloxymethyl)-3-hydroxy-5-methylpyrimidine-2,4(1H,3H)-dione (**54**).* This compound was prepared as a white solid following the procedure described for the preparation of **4**; yield 37%. ^{1}H NMR (600 MHz, $CDCl_3$) δ 7.32−7.28 (m, 5H), 7.06 (s, 1H), 5.25 (s, 2H), 4.60 (s, 2H), 1.93 (s, 3H). HRMS (ESI−) calcd for $C_{13}H_{14}N_2O_4$ $[M - H]^-$ 263.1026, found 263.1023 (E = 1.3 ppm).

*5-Benzyl-1-(benzyloxymethyl)-6-ethyl-3-hydroxypyrimidine-2,4(1H,3H)-dione (**55**).* This compound was prepared as a white solid following the procedure described for the preparation of **4**; yield 53%. ^{1}H NMR (600 MHz, $CDCl_3$) δ 7.22 (m, 4H), 7.19 (m, 3H), 7.12 (m, 3H), 5.42 (s, 2H), 4.61 (s, 2H), 3.76 (s, 2H), 2.68 (q, J = 7.2 Hz, 2H), 0.99 (t, J = 7.2 Hz, 3H). HRMS (ESI−) calcd for $C_{21}H_{22}N_2O_4$ $[M - H]^-$ 365.1507, found 365.1484 (E = 6.2 ppm).

*5-Benzyl-6-ethyl-1-((4-fluorobenzyloxy)methyl)-3-hydroxypyrimidine-2,4(1H,3H)-dione (**56**).* This compound was prepared as a white solid following the procedure described for the preparation of **4**; yield 59%. ^{1}H NMR (600 MHz, $CDCl_3$) δ 7.13 (m, 3H), 7.07 (m, 4H), 6.83 (t, J = 6.6 Hz, 2H), 5.28 (s, 2H), 4.48 (s, 2H), 3.67 (s, 2H), 2.72 (q, J = 6.6 Hz, 2H), 1.07 (t, J = 6.6 Hz, 3H). HRMS (ESI−) calcd for $C_{21}H_{21}FN_2O_4$ $[M - H]^-$ 383.1485, found 383.1394 (E = 4.8 ppm).

*1-Benzyl-6-(4-fluorobenzyl)-3-hydroxy-5-isopropylpyrimidine-2,4(1H,3H)-dione (**64**).* This compound was prepared as a white solid following the procedure described for the preparation of **4**; yield 70%. ^{1}H NMR (600 MHz, $CDCl_3$) δ 7.33 (t, J = 7.2 Hz, 2H), 7.30 (m, 1H), 7.11 (d, J = 7.2 Hz, 2H), 7.06−7.04 (m, 2H), 7.02−7.00 (m, 2H), 4.98 (s, 2H), 3.86 (s, 2H), 2.84 (septet, J = 7.2 Hz, 1H), 1.29 (d, J = 6.6 Hz, 6H). HRMS (ESI+) calcd for $C_{21}H_{21}FN_2O_3$ $[M + H]^+$ 369.1609, found 369.1606 (E = −1.9 ppm).

*1,6-Bis(4-fluorobenzyl)-3-hydroxy-5-isopropylpyrimidine-2,4(1H,3H)-dione (**65**).* This compound was prepared as a white solid following the procedure described for the preparation of **4**; yield 70%. ^{1}H NMR (600 MHz, $CDCl_3$) δ 7.10−7.08 (m, 2H), 7.06−7.04 (m, 2H), 7.02−6.99 (m, 4H), 4.94 (s, 2H), 3.89 (s, 2H), 2.84 (septet, J = 7.2 Hz, 1H), 1.28 (d, J = 6.6 Hz, 6H). ^{13}C NMR (150 MHz, $CDCl_3$) δ 163.1 (d, J = 31.2 Hz), 162.2, 161.4 (d, J = 31.2 Hz), 151.8, 148.3, 132.2 (d, J = 3.3 Hz), 130.4 (d, J = 2.9 Hz), 128.6 (d, J = 7.8 Hz), 127.6 (d, J = 8.4 Hz), 119.7, 116.4 (d, J = 21.8 Hz), 116.1 (d, J = 21.8 Hz), 46.6, 33.6, 28.2, 20.4. HRMS (ESI+) calcd for $C_{21}H_{20}F_2N_2O_3$ $[M + H]^+$ 387.1515, found 387.1502 (E = 3.3 ppm).

*1,6-Bibenzyl-3-hydroxy-5-isopropylpyrimidine-2,4(1H,3H)-dione (**66**).* This compound was prepared as a white solid following the procedure described for the preparation of **4**; yield 53%. ^{1}H NMR (600 MHz, $CDCl_3$) δ 7.39−7.34 (m, 4H), 7.32−7.30 (m, 2H), 7.12 (d, J = 7.2 Hz, 2H), 7.06 (d, J = 7.8 Hz, 2H), 5.00 (s, 2H), 3.91 (s, 2H), 2.90 (septet, J = 7.2 Hz, 1H), 1.29 (d, J = 7.2 Hz, 6H). HRMS (ESI+) calcd for $C_{21}H_{22}N_2O_3$ $[M + H]^+$ 351.1703, found 351.1689 (E = 4.1 ppm).

*1,6-Bibenzyl-5-ethyl-3-hydroxypyrimidine-2,4(1H,3H)-dione (**67**).* This compound was prepared as a white solid following the procedure described for the preparation of **4**; yield 43%. ^{1}H NMR (600 MHz, $CDCl_3$) δ 7.31−7.27 (m, 3H), 7.26−7.23 (m, 3H), 7.04 (d, J = 6.6 Hz, 2H), 7.00 (d, J = 6.6 Hz, 2H), 4.91 (s, 2H), 3.80 (s, 2H), 2.47 (q, J = 7.2 Hz, 2H), 1.00 (t, J = 7.2 Hz, 3H). HRMS (ESI+) calcd for $C_{20}H_{20}N_2O_3$ $[M + H]^+$ 337.1547, found 337.1534 (E = 3.8 ppm).

*6-Benzyl-5-ethyl-1-(4-fluorobenzyl)-3-hydroxypyrimidine-2,4(1H,3H)-dione (**68**).* This compound was prepared as a white solid following the procedure described for the preparation of **4**; yield 48%. ^{1}H NMR (600 MHz, $CDCl_3$) δ 7.38−7.35 (m, 2H), 7.32 (m, 1H), 7.15−7.13 (m, 2H), 7.07 (d, J = 7.8 Hz, 2H), 7.04 (m, 2H), 4.94 (s, 2H), 3.88 (s, 2H), 2.52 (q, J = 7.2 Hz, 2H), 1.07 (t, J = 7.2 Hz, 3H). HRMS (ESI+) calcd for $C_{20}H_{19}FN_2O_3$ $[M + H]^+$ 355.1452, found 355.1442 (E = 3.0 ppm).

*1-Benzyl-3-hydroxy-5-methylpyrimidine-2,4(1H,3H)-dione (**69**).* This compound was prepared as a white solid following the procedure described for the preparation of **4**; yield 32%. ^{1}H NMR (600 MHz, $CDCl_3$) δ 7.35−7.31 (m, 3H), 7.28 (d, J = 7.2 Hz, 2H), 6.94 (s, 1H), 4.94 (s, 2H), 1.90 (s, 3H). HRMS (ESI+) calcd for $C_{12}H_{12}N_2O_3$ $[M + H]^+$ 233.0921, found 233.0926 (E = −2.3 ppm).

*1-(4-Fluorobenzyl)-3-hydroxy-5-methylpyrimidine-2,4(1H,3H)-dione (**70**).* This compound was prepared as a white solid following the procedure described for the preparation of **4**; yield: 41%. ^{1}H NMR

(600 MHz, $CDCl_3$) δ 7.30−7.27 (m, 2H), 7.08−7.05 (m, 2H), 6.96 (s, 1H), 4.85 (s, 2H), 1.89 (s, 3H). HRMS (ESI−) calcd for $C_{12}H_{11}FN_2O_3$ $[M - H]^-$ 251.0826, found 251.0822 (E = 1.8 ppm).

Biology. *In Vitro Integrase Catalytic Assays.* Expression and purification of the recombinant IN in *Escherichia coli* were performed as previously reported[28,48] with addition of 10% glycerol to all buffers. Preparation of oligonucleotide substrates has been described.[49] Integrase reactions were performed in 10 μL with 400 nM of recombinant IN, 20 nM of 5′-end [^{32}P]-labeled oligonucleotide substrate, and inhibitors at various concentrations. Solutions of 10% DMSO without inhibitors were used as controls. Reactions were incubated at 37 °C (60 min) in buffer containing 50 mM MOPS, pH 7.2, 7.5 mM $MgCl_2$, and 14.3 mM 2-mercaptoethanol. Reactions were stopped by addition of 10 μL of loading dye (10 mM EDTA, 98% deionized formamide, 0.025% xylene cyanol, and 0.025% bromophenol blue). Reactions were then subjected to electrophoresis in 20% polyacrylamide−7 M urea gels. Gels were dried, and reaction products were visualized and quantitated with a Typhoon 8600 (GE Healthcare, Little Chalfont, Buckinghamshire, UK). Densitometric analyses were performed using ImageQuant from Molecular Dynamics Inc. The concentrations at which enzyme activity was reduced by 50% (IC_{50}) were determined using "Prism" software (GraphPad Software, San Diego, CA) for nonlinear regression to fit dose−response data to logistic curve models.

HIV-1 Assay. The HIV cytoprotection assay used CEM-SS cells and the IIIB strain of HIV-1. Briefly virus and cells were mixed in the presence of test compound and incubated for 6 days. The virus was pretitered such that control wells exhibit 70−95% loss of cell viability due to virus replication. Therefore, antiviral effect or cytoprotection was observed when compounds prevent virus replication. Each assay plate contained cell control wells (cells only), virus control wells (cells plus virus), compound toxicity control wells (cells plus compound only), and compound colorimetric control wells (compound only) as well as experimental wells (compound plus cells plus virus). Cytoprotection and compound cytotoxicity were assessed by MTS (CellTiter 96 Reagent, Promega, Madison WI) and the EC_{50} (concentration inhibiting virus replication by 50%), CC_{50} (concentration resulting in 50% cell death) and a calculated TI (therapeutic index CC_{50}/EC_{50}) were provided. Each assay included the HIV RT inhibitor AZT as a positive control.

Modeling and Docking. All modeling studies were carried out using the Schrodinger Modeling suite[50] based on our previous homology model[38] of HIV-1 IN CCD−DNA complex using Glide with standard precision protocol.[51] The Mg^{2+} ions and the interfacial hydrophobic pocket between the HIV-1 IN and DNA were defined as required constraints. The van der Waals radii of nonpolar atoms for each of the ligands were scaled by a factor of 0.8 to account for structure variability to specific ligand binding. Validation of the docking protocol was carried out by redocking both raltegravir and elvitegravir into the ligand binding site with structure comparison to the earlier reported mode of binding in PFV IN complex.[36] To further validate our structural model for HIV IN inhibitor design, correlation of the experimental and predicted IC_{50}s for a common mode of binding was performed for the most active compounds (**4**, **11**, **28**, **29**, **30**, **32**, **42**) based on the linear response method[52] implemented within Liason.[50]

■ ASSOCIATED CONTENT

Supporting Information. Additional experimental details and NMR, MS, and HPLC data for **31**, **34**−**41**, **57**−**63**, and **72**−**76**. This material is available free of charge via the Internet at http://pubs.acs.org.

■ AUTHOR INFORMATION

Corresponding Author

*Phone: +1 (612) 626-7025. Fax: +1 (612) 625-8154. E-mail: wangx472@umn.edu.

■ ACKNOWLEDGMENT

This research was supported by the Center for Drug Design at the University of Minnesota, the Center for Cancer Research, Intramural Program of the National Cancer Institute, and an NIH grant from IATAP (Intramural AIDS Targeted Antiviral Program). We thank Roger Ptak at Southern Research Institute for the antiviral assay and the Minnesota Supercomputing Institute for computing resources.

■ ABBREVIATIONS USED

IN, integrase; HIV, human immunodeficiency virus; INI, integrase inhibitor; SAR, structure−activity relationship; 3′P, 3′ processing; ST, strand transfer; DKA, diketoacid; HAART, highly active antiretroviral therapy; AIDS, acquired immunodeficiency syndrome; RT, reverse transcriptase; NTD, N-terminal domain; CCD, catalytic core domain; CTD, C-terminal domain; PFV, prototype foamy virus; *m*-CPBA, *meta*-chloroperbenzoic acid; CPE, cytopathic effect

■ REFERENCES

(1) Bagasra, O. A unified concept of HIV latency. *Expert Opin. Biol. Ther.* **2006**, *6*, 1135–1149.

(2) Chun, T.-W.; Stuyver, L.; Mizell, S. B.; Ehler, L. A.; Mican, J. A. M.; Baseler, M.; Lloyd, A. L.; Nowak, M. A.; Fauci, A. S. Presence of an inducible HIV-1 latent reservoir during highly active antiretroviral therapy. *Proc. Natl. Acad. Sci. U.S.A.* **1997**, *94*, 13193–13197.

(3) Finzi, D.; Hermankova, M.; Pierson, T.; Carruth, L. M.; Buck, C.; Chaisson, R. E.; Quinn, T. C.; Chadwick, K.; Margolick, J.; Brookmeyer, R.; Gallant, J.; Markowitz, M.; Ho, D. D.; Richman, D. D.; Siliciano, R. F. Identification of a reservoir for HIV-1 in patients on highly active antiretroviral therapy. *Science* **1997**, *278*, 1295–1300.

(4) Engelman, A.; Mizuuchi, K.; Craigie, R. HIV-1 DNA integration: mechanism of viral DNA cleavage and DNA strand transfer. *Cell* **1991**, *67*, 1211–1221.

(5) Pommier, Y.; Johnson, A. A.; Marchand, C. Integrase inhibitors to treat HIV/AIDS. *Nature Rev. Drug Discovery* **2005**, *4*, 236–248.

(6) Cotelle, P. Patented HIV-1 integrase inhibitors (1998−2005). *Recent Pat. Anti-Infect. Drug Discovery* **2006**, *1*, 1–15.

(7) Henao-Mejia, J.; Goez, Y.; Patino, P.; Rugeles, M. T. Diketo acids derivatives as integrase inhibitors: the war against the acquired immunodeficiency syndrome. *Recent Pat. Anti-Infect. Drug Discovery* **2006**, *1*, 255–265.

(8) Dubey, S.; Satyanarayana, Y. D.; Lavania, H. Development of integrase inhibitors for treatment of AIDS: an overview. *Eur. J. Med. Chem.* **2007**, *42*, 1159–1168.

(9) Marchand, C.; Maddali, K.; Metifiot, M.; Pommier, Y. HIV-1 IN inhibitors: 2010 update and perspectives. *Curr. Top. Med. Chem.* **2009**, *9*, 1016–1037.

(10) Dayam, R.; Sanchez, T.; Neamati, N. Diketo Acid Pharmacophore. 2. Discovery of Structurally Diverse Inhibitors of HIV-1 Integrase. *J. Med. Chem.* **2005**, *48*, 8009–8015.

(11) Dayam, R.; Sanchez, T.; Clement, O.; Shoemaker, R.; Sei, S.; Neamati, N. β-Diketo acid pharmacophore hypothesis. 1. Discovery of a novel class of HIV-1 integrase inhibitors. *J. Med. Chem.* **2005**, *48*, 111–120.

(12) Deng, J.; Sanchez, T.; Neamati, N.; Briggs, J. M. Dynamic Pharmacophore Model Optimization: Identification of Novel HIV-1 Integrase Inhibitors. *J. Med. Chem.* **2006**, *49*, 1684–1692.

(13) Barreca, M. L.; Ferro, S.; Rao, A.; De Luca, L.; Zappala, M.; Monforte, A.-M.; Debyser, Z.; Witvrouw, M.; Chimirri, A. Pharmacophore-Based Design of HIV-1 Integrase Strand-Transfer Inhibitors. *J. Med. Chem.* **2005**, *48*, 7084–7088.

(14) Mustata, G. I.; Brigo, A.; Briggs, J. M. HIV-1 integrase pharmacophore model derived from diverse classes of inhibitors. *Bioorg. Med. Chem. Lett.* **2004**, *14*, 1447–1454.

(15) Carlson, H. A.; Masukawa, K. M.; Rubins, K.; Bushman, F. D.; Jorgensen, W. L.; Lins, R. D.; Briggs, J. M.; McCammon, J. A. Developing a Dynamic Pharmacophore Model for HIV-1 Integrase. *J. Med. Chem.* **2000**, *43*, 2100–2114.

(16) Cocohoba, J.; Dong, B. J. Raltegravir: the first HIV integrase inhibitor. *Clin. Ther.* **2008**, *30*, 1747–1765.
(17) Summa, V.; Petrocchi, A.; Bonelli, F.; Crescenzi, B.; Donghi, M.; Ferrara, M.; Fiore, F.; Gardelli, C.; Gonzalez Paz, O.; Hazuda, D. J.; Jones, P.; Kinzel, O.; Laufer, R.; Monteagudo, E.; Muraglia, E.; Nizi, E.; Orvieto, F.; Pace, P.; Pescatore, G.; Scarpelli, R.; Stillmock, K.; Witmer, M. V.; Rowley, M. Discovery of Raltegravir, a Potent, Selective Orally Bioavailable HIV-Integrase Inhibitor for the Treatment of HIV−AIDS Infection. *J. Med. Chem.* **2008**, *51*, 5843–5855.
(18) Shimura, K.; Kodama, E. N. Elvitegravir: a new HIV integrase inhibitor. *Antiviral Chem. Chemother.* **2009**, *20*, 79–85.
(19) Vandekerckhove, L. GSK-1349572, a novel integrase inhibitor for the treatment of HIV infection. *Curr. Opin. Invest. Drugs* **2010**, *11*, 203–212.
(20) Min, S.; Song, I.; Borland, J.; Chen, S.; Lou, Y.; Fujiwara, T.; Piscitelli, S. C. Pharmacokinetics and safety of S/GSK1349572, a next-generation HIV integrase inhibitor, in healthy volunteers. *Antimicrob. Agents Chemother.* **2009**, *54*, 254–258.
(21) Prada, N.; Markowitz, M. Novel integrase inhibitors for HIV. *Expert Opin Invest. Drugs* **2010**, *19*, 1087–1098.
(22) Cherepanov, P.; Ambrosio, A. L. B.; Rahman, S.; Ellenberger, T.; Engelman, A. Structural basis for the recognition between HIV-1 integrase and transcriptional coactivator p75. *Proc. Natl. Acad. Sci. U.S.A.* **2005**, *102*, 17308–17313.
(23) Hombrouck, A.; De Rijck, J.; Hendrix, J.; Vandekerckhove, L.; Voet, A.; De Maeyer, M.; Witvrouw, M.; Engelborghs, Y.; Christ, F.; Gijsbers, R.; Debyser, Z. Virus evolution reveals an exclusive role for LEDGF/p75 in chromosomal tethering of HIV. *PLoS Pathog.* **2007**, *3*, 418–430.
(24) Engelman, A. Host cell factors and HIV-1 integration. *Future HIV Ther.* **2007**, *1*, 415–426.
(25) Christ, F.; Voet, A.; Marchand, A.; Nicolet, S.; Desimmie, B. A.; Marchand, D.; Bardiot, D.; Van der Veken, N. J.; Van Remoortel, B.; Strelkov, S. V.; De Maeyer, M.; Chaltin, P.; Debyser, Z. Rational design of small-molecule inhibitors of the LEDGF/p75-integrase interaction and HIV replication. *Nature Chem. Biol.* **2010**, *6*, 442–448.
(26) Yeni, P. Update on HAART in HIV. *J. Hepatol.* **2006**, *44*, S100–S103.
(27) Metifiot, M.; Marchand, C.; Maddali, K.; Pommier, Y. Resistance to integrase inhibitors. *Viruses* **2010**, *2*, 1347–1366.
(28) Metifiot, M.; Maddali, K.; Naumova, A.; Zhang, X.; Marchand, C.; Pommier, Y. Biochemical and Pharmacological Analyses of HIV-1 Integrase Flexible Loop Mutants Resistant to Raltegravir. *Biochemistry* **2010**, *49*, 3715–3722.
(29) da Silva, D.; Van Wesenbeeck, L.; Breilh, D.; Reigadas, S.; Anies, G.; Van Baelen, K.; Morlat, P.; Neau, D.; Dupon, M.; Wittkop, L.; Fleury, H.; Masquelier, B. HIV-1 resistance patterns to integrase inhibitors in antiretroviral-experienced patients with virological failure on raltegravir-containing regimens. *J. Antimicrob. Chemother.* **2010**, *65*, 1262–1269.
(30) Tang, J.; Maddali, K.; Dreis, C. D.; Sham, Y. Y.; Vince, R.; Pommier, Y.; Wang, Z. N-3 Hydroxylation of Pyrimidine-2,4-diones Yields Dual Inhibitors of HIV Reverse Transcriptase and Integrase. *ACS Med. Chem. Lett.* **2011**, *2*, 63–67.
(31) Esposito, D.; Craigie, R. HIV integrase structure and function. *Adv. Virus Res.* **1999**, *52*, 319–333.
(32) Goldgur, Y.; Dyda, F.; Hickman, A. B.; Jenkins, T. M.; Craigie, R.; Davies, D. R. Three new structures of the core domain of HIV-1 integrase: an active site that binds magnesium. *Proc. Natl. Acad. Sci. U.S. A.* **1998**, *95*, 9150–9154.
(33) Dyda, F.; Hickman, A. B.; Jenkins, T. M.; Engelman, A.; Craigie, R.; Davies, D. R. Crystal structure of the catalytic domain of HIV-1 integrase: similarity to other polynucleotidyl transferases. *Science* **1994**, *266*, 1981–1986.
(34) O'Brien, C. HIV Integrase Structure Catalyzes Drug Search. *Science* **1994**, *266*, 1946.
(35) Alian, A.; Griner, S. L.; Chiang, V.; Tsiang, M.; Jones, G.; Birkus, G.; Geleziunas, R.; Leavitt, A. D.; Stroud, R. M. Catalytically-active complex of HIV-1 integrase with a viral DNA substrate binds anti-integrase drugs. *Proc. Natl. Acad. Sci. U.S.A.* **2009**, *106*, 8192–8197.
(36) Hare, S.; Gupta, S. S.; Valkov, E.; Engelman, A.; Cherepanov, P. Retroviral intasome assembly and inhibition of DNA strand transfer. *Nature* **2010**, *464*, 232–236.
(37) Hare, S.; Vosb, A. M.; Claytonb, R. F.; Thuringb, J. W.; Cummingsb, M. D.; Cherepanov, P. Molecular mechanisms of retroviral integrase inhibition and the evolution of viral resistance. *Proc. Natl. Acad. Sci. U.S.A.* **2010**, *107*, 20057–20062.
(38) Tang, J.; Maddali, K.; Pommier, Y.; Sham, Y. Y.; Wang, Z. Scaffold rearrangement of dihydroxypyrimidine inhibitors of HIV integrase: docking model revisited. *Bioorg. Med. Chem. Lett.* **2010**, *20*, 3275–3279.
(39) Krishnan, L.; Li, X.; Naraharisetty, H. L.; Hare, S.; Cherepanov, P.; Engelman, A. Structure-based modeling of the functional HIV-1 intasome and its inhibition. *Proc. Natl. Acad. Sci. U.S.A.* **2010**, *107*, 15910–15915.
(40) Tanaka, H.; Hayakawa, H.; Haraguchi, K.; Miyasaka, T.; Walker, R. T.; De Clercq, E.; Baba, M.; Stammers, D. K.; Stuart, D. I. HEPT: from an investigation of lithiation of nucleosides towards a rational design of non-nucleoside reverse transcriptase inhibitors of HIV-1. *Adv. Antiviral Drug Des.* **1999**, *3*, 93–144.
(41) Pontikis, R.; Benhida, R.; Aubertin, A.-M.; Grierson, D. S.; Monneret, C. Synthesis and Anti-HIV Activity of Novel N-1 Side Chain-Modified Analogs of 1-[(2-Hydroxyethoxy)methyl]-6-(phenylthio)-thymine (HEPT). *J. Med. Chem.* **1997**, *40*, 1845–1854.
(42) Tanaka, H.; Takashima, H.; Ubasawa, M.; Sekiya, K.; Inouye, N.; Baba, M.; Shigeta, S.; Walker, R. T.; Clercq, E. D.; Miyasaka, T. Synthesis and Antiviral Activity of 6-Benzyl Analogs of 1-[(2-Hydroxyethoxy)methyl]-5-(phenylthio)thymine (HEPT) as Potent and Selective Anti-HIV-1 Agents. *J. Med. Chem.* **1995**, *38*, 2860–2865.
(43) Tanaka, H.; Baba, M.; Hayakawa, H.; Sakamaki, T.; Miyasaka, T.; Ubasawa, M.; Takashima, H.; Sekiya, K.; Nitta, I.; Shigeta, S.; Walker, R. T.; Balzarini, J.; Clercq, E. D. A new class of HIV-1 specific 6-substituted acyclouridine derivatives: synthesis and anti-HIV-1 activity of 5- or 6-substituted analogs of 1-[(2-hydroxyethoxy)methyl]-6-(phenylthio)thymine (HEPT). *J. Med. Chem.* **1991**, *34*, 349–357.
(44) Wang, Z.; Bennett, E. M.; Wilson, D. J.; Salomon, C.; Vince, R. Rationally Designed Dual Inhibitors of HIV Reverse Transcriptase and Integrase. *J. Med. Chem.* **2007**, *50*, 3416–3419.
(45) Danel, K.; Larsen, E.; Pedersen, E. B.; Vestergaard, B. F.; Nielsen, C. Synthesis and Potent Anti-HIV-1 Activity of Novel 6-Benzyluracil Analogs of 1-[(2-Hydroxyethoxy)methyl]-6-(phenylthio)-thymine. *J. Med. Chem.* **1996**, *39*, 2427–2431.
(46) These assays were done in MAGI R5 cells with NNRTI TNK-651 as a control. The observed fold-resistances for the control were 22 and 72 for K103N and Y181C mutants.
(47) Bernardes, G. J. L.; Chalker, J. M.; Errey, J. C.; Davis, B. G. Facile Conversion of Cysteine and Alkyl Cysteines to Dehydroalanine on Protein Surfaces: Versatile and Switchable Access to Functionalized Proteins. *J. Am. Chem. Soc.* **2008**, *130*, 5052–5053.
(48) Leh, H.; Brodin, P.; Bischerour, J.; Deprez, E.; Tauc, P.; Brochon, J. C.; LeCam, E.; Coulaud, D.; Auclair, C.; Mouscadet, J. F. Determinants of Mg^{2+}-dependent activities of recombinant human immunodeficiency virus type 1 integrase. *Biochemistry* **2000**, *39*, 9285–9294.
(49) Semenova, E. A.; Johnson, A. A.; Marchand, C.; Davis, D. A.; Yarchoan, R.; Pommier, Y. Preferential inhibition of the magnesium-dependent strand transfer reaction of HIV-1 integrase by α-hydroxytropolones. *Mol. Pharmacol.* **2006**, *69*, 1454–1460.
(50) Maestro version 9.1, G version; Macromodel version 9.8; Liason version 5.6, version 9.1; Schrodinger, LLC: New York.
(51) Friesner, R. A.; Banks, J. L.; Murphy, R. B.; Halgren, T. A.; Klicic, J. J.; Mainz, D. T.; Repasky, M. P.; Knoll, E. H.; Shelley, M.; Perry, J. K.; Shaw, D. E.; Francis, P.; Shenkin, P. S. Glide: a new approach for rapid, accurate docking and scoring. 1. Method and assessment of docking accuracy. *J. Med. Chem.* **2004**, *47*, 1139–1149.
(52) Hansson, T.; Aqvist, J. Estimation of binding free energies for HIV proteinase inhibitors by molecular dynamics simulations. *Protein Eng.* **1995**, *8*, 1137–1144.

NOTE ADDED AFTER ASAP PUBLICATION

An author name was inadvertently omitted in the version of this paper published ASAP on March 7, 2011. The corrected version was reposted on March 14, 2011.